Доклади на Българската академия на науките
Comptes rendus de l'Académie bulgare des Sciences
Tome 76, No 10, 2023

MEDICINE

Clinical medicine

TEXTURE ANALYSIS OF ADENOMATOUS AND METASTATIC ADRENAL LESIONS ON NATIVE AND CONTRAST-ENHANCED COMPUTED TOMOGRAPHY

Magdalena Belyanova, Martin Krupev

Received on September 29, 2020
Presented by D. Damianov, Member of BAS, on October 29, 2020

Abstract

Differentiating lipid-poor adrenal adenomas from adrenal metastases is not possible without performing a dedicated contrast-enhanced CT (CECT) protocol. Our purpose is to evaluate the possible role of texture analysis in classifying adrenal lesions.

This is a retrospective study. We evaluated 33 patients with 47 metastases and 43 patients with 47 adenomas. Seven of the adenomas were lipid-poor, and the rest – lipid-rich adenomas. We used commercially available software for lesion segmentation and texture analysis on native and arterial phase CT images with a slice thickness of 2 mm. The segmentation was semi-automated, and features were computed on the resulting regions of interest (ROI) for each lesion on both native and arterial phases. Two conventional (HU standard deviation, Histogram Entropy) and six second-order texture features (GLCM – Homogeneity, Energy, Entropy log 10, Contrast, Dissimilarity, NGDLM–Busyness) were calculated. For statistical analysis the IBM SPSS 19 package was used to compare the following groups in both phases: 1. Adenomas–Metastasis; 2. Lipid-rich adenomas (LRA)–metastases; 3. Lipid-rich–lipid-poor adenomas (LPA); 4. Lipid-poor adenomas–metastases.

There was a statistically significant difference in the distribution of some conventional (Histogram Entropy) and second-order features (GLCM – Homogeneity, Energy, Entropy log 10, Dissimilarity) in the first group on the native as well as on the enhanced images. The results were similar when comparing lipid-rich adenomas to metastases. Only native phase derived features were

DOI:10.7546/CRABS.2023.10.16

discriminative between lipid-rich and lipid-poor adenomas, with no difference between parameters on CECT. No difference was found between any of the texture features in lipid-poor adenomas and metastases for both phases.

First- and second-order texture features were graded based on their potential for serving as classifier tools. Unenhanced features ranked higher. Further research and validation are needed to discover the most robust set of features for differentiating between lipid-poor adenomas and metastases.

Key words: lipid-poor adrenal adenoma, adrenal metastasis, texture analysis

Introduction. Adrenal lesions are a frequent incidental imaging finding, reported to be present in approximately 2% of studies, performed for different reasons [1]. Even in patients with known malignancy, most adrenal nodules histologically represent adenomas. Oliver et al. [13] assessed adrenal lesions in patients with lung cancer and found that 68% of the lesions were adenomas. Accurate adrenal mass characterization is of importance in the newly discovered cancer patient for adequate staging and management. Misclassification of an adenoma as metastasis may detain patients from radical cancer treatment, whereas treating a metastatic lesion as benign may lead to unnecessary surgery. Computed tomography (CT) is the gold standard for adrenal lesion characterization. Due to the high intracellular lipid content, most adenomas have a mean attenuation value on unenhanced CT of < 10 HU [9]. Unfortunately, nearly $1/3$ of all adenomas are "lipid-poor" adenomas which do not meet this criterion.

Korobkin et al. [8] have developed a dedicated CT protocol for diagnosing adenomas based on their propensity for rapid washout after contrast administration. The protocol consists of native phase and additional scans at 60 s and 15 min post injection. Potential drawbacks in everyday practice include the need for timely diagnosis of an incidentaloma; the need for contrast administration; the increase in overall study duration.

Texture analysis is a rapidly evolving method in oncology for extracting, analyzing, and interpreting quantitative features from medical images [10]. This method allows quantification of image heterogeneity and has shown promising results in lesion categorization [2, 11], in the prognosis of progression, and in predicting histology and genotype [3, 5]. It can be applied as a post-processing step in a variety of different medical images. Statistical methods for texture assessment generate features of different orders which differ in their approach to describing voxel distribution in the ROI. First-order features are histogram-based and calculate the frequency with which different gray-level voxels are encountered in the ROI, without accounting for their position in space [14]. HISTO_Entropy_log10 is a first-order feature expressing the randomness of the gray level frequency distribution. Second-order texture features are the most frequently utilized for heterogeneity assessment. They take into account the spatial relationship between different gray level voxels. These features are calculated from a set of matrices

including the Gray-level co-occurrence matrix (GLCM), Grey level run-length matrix (GLRLM), neighbourhood grey-level difference matrix (NGLDM), grey-level zone length matrix (GLZLM). GLCM expresses the spatial relationship between adjacent voxels with a certain intensity. It is a numerical matrix with numbers representing the frequency with which a pair of voxels with predefined intensity and offset are encountered in the ROI [6]. NGLDM "corresponds to the difference of grey-levels between one voxel and its 26 neighbours in 3 dimensions", according to Nioche et al. [12].

Materials and methods. Seventy-eight patients with 94 adrenal nodules examined between August 2016 and August 2020 were retrospectively selected from our institution's Picture Archiving and Communication System (PACS). All patients underwent a CT examination with the same 64 slice Toshiba Aquilion scanner. Scan parameters used were: 120 kVp; variable tube current with automatic tube current modulation activated; rotation time 0.5 s and pitch=1.484. For the post-processing, we used images with a slice thickness of 2 mm in native and arterial phases. Arterial phase images were acquired 30 s after application of 100 ml contrast material (Ultravist 370) with an injection rate of 3–3.5 ml/s.

The age range was 41–80 years, mean age – 65 years. Lesions were deemed metastatic when they had a mean density of > 10 HU on native phase in a patient with known neoplasm. Exclusion criteria were size less than 10 mm and grossly necrotic lesions. The resultant group consisted of 33 patients with 47 metastatic lesions.

The group of adenomas consisted of 43 patients with 47 lesions, which were divided into two subgroups:

- Lipid-rich adenomas (LRA, 40 lesions) – in patients with an adrenal nodule with a mean density < 10 HU, with or without concomitant neoplasm;
- Lipid-poor adenoma (LPA, 7 lesions) – lesions with a mean density > 10 HU in patients without concomitant neoplasm.

For image post-processing, we used the LIFEx commercially available software [12]. Lesion segmentation was semi-automated and generated 3D ROIs. Care was taken not to include calcifications, vessels, and lesion margins (Fig. 1). Intensity discretization was performed with fixed bin number (64) and absolute rescaling between -150 and $+300$ HU. For each lesion two conventional (mean density standard deviation, HISTO_Entropy_log10) and six second-order features from the GLCM (Homogeneity, Energy, Contrast, Entropy, Dissimilarity) and NGLDM (Busyness) were calculated. Features were extracted for both native and enhanced images. IBM SPSS 19 software package was used to compare the obtained values between the following groups in both phases: 1. Adenomas–Metastasis; 2. LRA–metastases; 3. LRA–LPA; 4. LPA-metastases. A Bonferroni correction was done resulting in $P < 0.00625$.

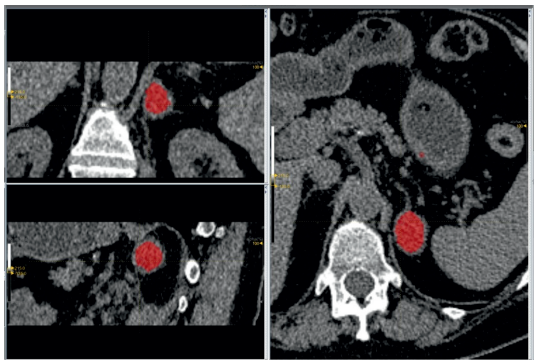


Fig. 1. A 3D ROI was drawn for each lesion in both phases and was used for calculation of features

Results. ***1. Adenomas–Metastasis*:** Results of the Mann–Whitney U test demonstrated a statistically significant difference in the distribution of first-order (HISTO_Entropy) and second-order (Homogeneity, Energy, Contrast, Entropy, Dissimilarity) mean ranks between adenomas and metastases on both phases. Effect size (d values) ranged from 1.9 (GLCM entropy) to 2 (Histo_Entropy) in the native phase and from 1.6 (GLCM Entropy) and 1.8 (HISTO_Entropy) in the arterial phase.

***2. LRA–metastases*:** There was a significant difference between the mean ranks of HISTO_Entropy, GLCM Homogeneity, Energy, Contrast, Entropy and Dissimilarity in LRA and metastases on both phases with d ranging from 1.9 (GLCM Entropy) to 2.06 (Histo Entropy) on native phase features and from 1.65 (GLCM Entropy) to 2 (GLCM Homogeneity, Dissimilarity) in the arterial phase.

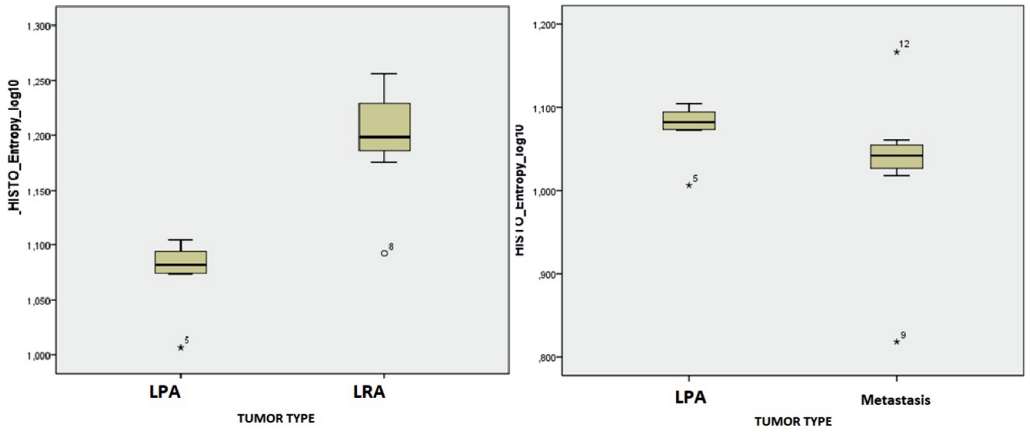


Fig. 2. Box plots of Histo Entropy value distribution compared between LPA and LRA on the left and LPA and metastases on the right

***3. LRA–LPA*:** The results showed differences in HISTO_Entropy, GLCM Homogeneity, Energy, and Entropy values in the native phase, d values were 2.16 for GLCM Homogeneity, and 2.4 for the remainder. No difference was evident between features calculated from arterial phase images.

***4. LPA-metastases*:** The results from the nonparametric test failed to demonstrate a significant difference across all 8 texture features.

Discussion. Two first-order and six second-order texture features were assessed for robustness. Both native and arterial phase parameters were evaluated since they are known to reflect separate tumour qualities. Native images provide insight into tumour histology, whereas contrast-enhanced images express tumour vascularity.

LRA and metastases demonstrated significant differences in both enhanced and unenhanced texture features, with Histo Entropy being the best performing feature. LRA and LPA showed significant differences in their native phase parameters which were mitigated when comparing arterial phase features. Ho et al. [6] explained this phenomenon in their paper. They studied 15 LPA and 8 malignant masses by comparing 21 second-order features derived from NECT, venous phase CT and MRI. The researchers observed a significant difference between 9 native and 18 venous phase features including GLCM derivatives. It was postulated that both types of lesions have inherent heterogeneity, which is due to the uneven distribution of lipid-poor and lipid-rich cell populations in LPA, and areas of necrosis and calcification in tumours. The authors theorized that contrast administration erases regional differences in adenomas because both cell populations have the same vascularity.

Our study group did not demonstrate a statistically significant difference between the mean ranks of features in LPA and metastases. P values were > 0.00625 for both phases with native features having lower values. These results conflict with some previously reported findings [6, 18]. One possible explanation could lie in the small sample size (7) which prompted us to use a non-parametric statistical test with lower statistical power. We calculated local texture maps for each subgroup of adrenal lesions to discern if our findings were associated with the statistical test or the raw data were originally similar. Local texture maps are visually intuitive means for expressing texture features. LPA and metastases showed similar maps, whereas LRA had a coarser structure (Fig. 3). These observations support the results of the Mann–Whitney U test.

With the help of current software and computer-assisted techniques multiple texture features can be calculated. Many of these are closely correlated with each other and prove redundant. Several authors have used different order texture features which were not discriminative by themselves but when used in conjunction as input for different algorithms achieved satisfactory sensitivity and specificity when differentiating LPA from metastases [4, 7, 15–18]. There is no consensus on which combination of features provides the best results. Ranking features based on their

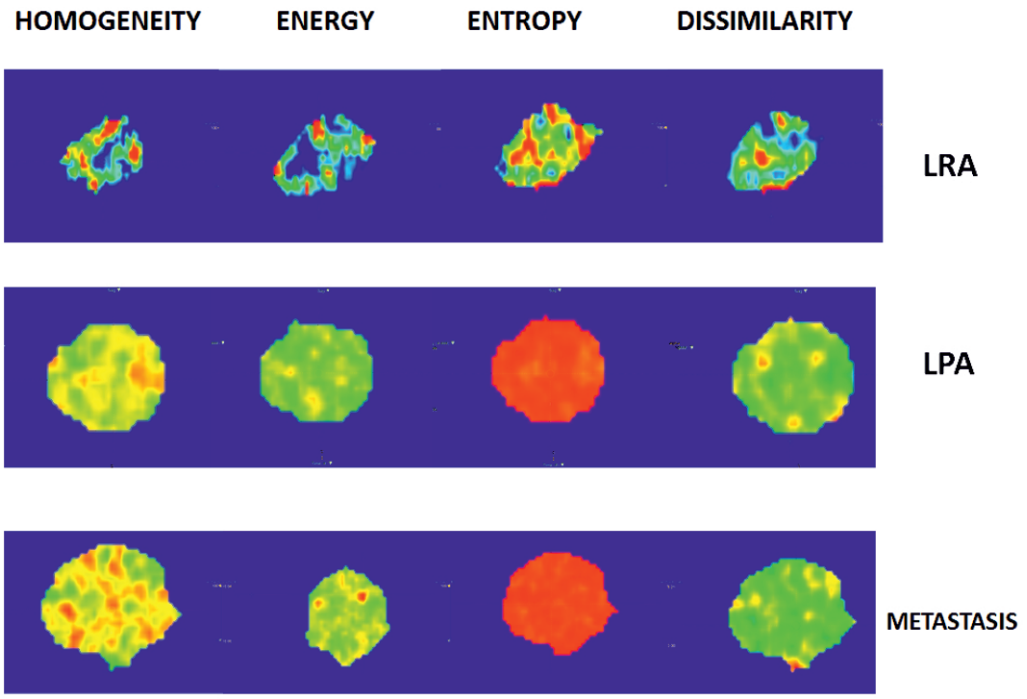


Fig. 3. Local texture maps for GLCM derived features show a similarity between LPA and metastases

potential discriminative power may prove more helpful than finding a single robust feature. The current study found first-order Histo Entropy and second-order GLCM Homogeneity, Energy, Entropy to have higher discriminative potential, followed by GLCM Contrast and Dissimilarity. NGLDM Busyness ranked lowest. Non-enhanced features ranked higher for all compared groups.

Romeo et al. [15] explored texture analysis in a group of 60 patients (20 LPA, 20 LRA, and 20 non-adenomatous lesions (NAL). They calculated 138 texture features. The best performing features were used to train an algorithm that achieved a diagnostic accuracy of 80%. In their study, first order and long-run emphasis (RLM) features outperformed GLCM derivatives. First-order features proved to be more robust. Our experience supports these findings. Histogram Entropy was found to be the highest-ranking texture feature in terms of effect size. It showed a lower mean rank in metastases in comparison with LRA. Although not statistically significant Histogram energy was still lower in metastases compared to LPA. Previous studies have demonstrated similar lower mean values of this feature in malignant tumors [6]. One recent study by Shi et al. [16] assessed 265 histologically proven masses (including 66 LPA and 101 metastases) on native and venous phase CT images. Entropy was among the six histogram-derived NECT features and four CECT features, which showed lower values in metastases.

This study has several contributions. To our knowledge, it is the first study to compare texture features among LRA-LPA, and LRA-metastases. It is also one of the few studies of texture analysis to use arterial phase images. We used whole tumour volume thus achieving a higher level of confidence. Limitations of this study include its retrospective nature. The final diagnosis was based on a combination of clinical and imaging findings of benignity which may lead to misclassification. We did not perform spatial resampling and no filter was applied. Bigger study groups are needed to confirm the presented findings. Validation of the selected features as a classifying tool is the subject of future work.

Conclusion. First- and second-order texture features were graded based on their potential for serving as classifier tools. Unenhanced features ranked higher. Further research and validation are needed to discover the most robust set of features for differentiating between lipid-poor adenomas and metastases.

REFERENCES

[1] Barzon L., N. Sonino, F. Fallo et al. (2003) Prevalence and natural history of adrenal incidentalomas, Eur. J. Endocrinol., **149**(4), 273–285.

[2] Cui C., H. Cai, L. Liu et al. (2011) Quantitative analysis and prediction of regional lymph node status in rectal cancer based on computed tomography imaging, Eur. Radiol., **21**(11), 2318–2325.

[3] El Naqa I., P. Grigsby, A. Apte et al. (2009) Exploring feature-based approaches in PET images for predicting cancer treatment outcomes, Pattern Recognit., **42**(6), 1162–1171.

[4] Elmohr M. M., D. Fuentes, M. A. Habra et al. (2019) Machine learning-based texture analysis for differentiation of large adrenal cortical tumours on CT, Clin. Radiol., **74**(10), 818.e1–818.e7.

[5] Goh V., B. Ganeshan, P. Nathan et al. (2011) Assessment of response to tyrosine kinase inhibitors in metastatic renal cell cancer: CT texture as a predictive biomarker, Radiology, **261**(1), 165–171.

[6] Ho L. M., E. Samei, M. A. Mazurowski et al. (2019) Can texture analysis be used to distinguish benign from malignant adrenal nodules on unenhanced CT, contrast-enhanced CT, or in-phase and opposed-phase MRI?, Am. J. Roentgen., **212**(3), https://doi.org/10.2214/AJR.18.20097.

[7] Hodgdon T., M. D. F. McInnes, N. Schieda et al. (2015) Can quantitative CT texture analysis be used to differentiate fat-poor renal angiomyolipoma from renal cell carcinoma on unenhanced CT images?, Radiology, **276**(3), 787–796.

[8] Korobkin M., F. J. Brodeur, I. R. Francis et al. (1998) CT time-attenuation washout curves of adrenal adenomas and nonadenomas, Am. J. Roentg., **170**(3), 747–752.

[9] Lee M. J., P. F. Hahn, N. Papanicolaou et al. (1991) Benign and malignant adrenal masses: CT distinction with attenuation coefficients, size, and observer analysis, Radiology, **179**(2), 415–418.

[10] Lubner M. G., A. D. Smith, K. Sandrasegaran et al. (2017) CT texture analysis: Definitions, applications, biologic correlates, and challenges, Radiographics, **37**(5), 1483–1503.
[11] Mayerhoefer M. E., M. Breitenseher, G. Amann, M. Dominkus (2008) Are signal intensity and homogeneity useful parameters for distinguishing between benign and malignant soft tissue masses on MR images? Objective evaluation by means of texture analysis, Magn. Reson. Imaging, **26**(9), 1316–1322.
[12] Nioche C., F. Orlhac, S. Boughdad et al. (2018) LIFEx: A freeware for radiomic feature calculation in multimodality imaging to accelerate advances in the characterization of tumor heterogeneity, Cancer Res., **78**(16), 4786–4789.
[13] Oliver T. W., Jr., M. E. Bernardino, J. I. Miller et al. (1984) Isolated adrenal masses in nonsmall-cell bronchogenic carcinoma, Radiology, **153**(1), 217–218.
[14] Ranjbar S., J. Ross Mitchell (2017) An introduction to radiomics: An evolving cornerstone of precision medicine. In: Biomedical Texture Analysis: Fundamentals, Tools and Challenges (eds A. Depeursinge, O. S. Al-Kadi, J. Ross Mitchell), Academic Press, 223–245, ISBN 9780128121337.
[15] Romeo V., S. Maurea, R. Cuocolo et al. (2018) Characterization of adrenal lesions on unenhanced MRI using texture analysis: A machine-learning approach, J. Magn. Reson. Imaging, **48**(1), 198–204.
[16] Shi B., G. M. Y. Zhang, M. Xu et al. (2019) Distinguishing metastases from benign adrenal masses: what can CT texture analysis do?, Acta Radiol., **60**(11), 1553–1561.
[17] Yi X., X. Guan, C. Chen et al. (2018) Adrenal incidentaloma: Machine learning-based quantitative texture analysis of unenhanced CT can effectively differentiate sPHEO from lipid-poor adrenal adenoma, J. Cancer, **9**(19), 3577–3582.
[18] Yi X., X. Guan, Y. Zhang et al. (2018) Radiomics improves efficiency for differentiating subclinical pheochromocytoma from lipid-poor adenoma: a predictive, preventive and personalized medical approach in adrenal incidentalomas, EPMA J., **9**(4), 421–429.

Medical University – Sofia
UMHAT "Alexandrovska"
1 St. G. Sofiiski St
1431 Sofia, Bulgaria
e-mail: mbelyanova@yahoo.com
krupev@yahoo.com